J. Korean Math. Soc. **58** (2021), No. 4, pp. 835–847
https://doi.org/10.4134/JKMS.j200257
pISSN: 0304-9914 / eISSN: 2234-3008

NUMERICAL SOLUTIONS FOR ONE AND TWO DIMENSIONAL NONLINEAR PROBLEMS RELATED TO DISPERSION MANAGED SOLITONS

Younghoon Kang, Eunjung Lee, and Young-Ran Lee

Abstract. We study behavior of numerical solutions for a nonlinear eigenvalue problem on $\mathbb{R}^n$ that is reduced from a dispersion managed nonlinear Schrödinger equation. The solution operator of the free Schrödinger equation in the eigenvalue problem is implemented via the finite difference scheme, and the primary nonlinear eigenvalue problem is numerically solved via Picard iteration. Through numerical simulations, the results known only theoretically, for example the number of eigenpairs for one dimensional problem, are verified. Furthermore several new characteristics of the eigenpairs, including the existence of eigenpairs inherent in zero average dispersion two dimensional problem, are observed and analyzed.

1. Introduction

Dispersion management systems are widely used in optical business with various applications. Primarily, they are utilized to find a fast and stable manner to transfer data through fiber-optic cables over long distance. In fact, such optical systems have facilitated almost zero path-averaged dispersion curtailing pulse widening, and an actual experimental result had demonstrated the effects of this technique in [24]. Nowadays, numerous numerical researches on nonlinear Schrödinger equation related to the same field are still active [3, 22].

This paper focuses on numerical study of unsolved theoretical characteristics related to the following nonlinear problem, known as the dispersion managed nonlinear Schrödinger equation (DM NLS):

$$i\partial_t u + d(t)\nabla^2 u + |u|^2 u = 0, \tag{1}$$

where the Laplacian ∇^2 is either ∂_x^2 in $\mathbb{R}$ or $\partial_{x_1}^2 + \partial_{x_2}^2$ in $\mathbb{R}^2$. Here $t \in \mathbb{R}$ describes the distance along the fiber-optic cable. For $x \in \mathbb{R}$, x is the retarded

Received May 9, 2020; Revised September 12, 2020; Accepted September 21, 2020.
2010 *Mathematics Subject Classification.* 78M20, 65M06.
Key words and phrases. Schrodinger equation, numerical solution, eigenvalue problem.
Young-Ran Lee and Eunjung Lee were supported by the National Research Foundation of Korea, NRF-2017R1D1A1B03033939 and NRF-2018R1D1A1B07042973, respectively.

time, while $\mathbf{x} := (x_1, x_2) \in \mathbb{R}^2$ is the coordinate of the section orthogonal to the fiber. The function $d(t)$ is defined as

$$d(t) = \frac{1}{\varepsilon} d_0\left(\frac{t}{\varepsilon}\right) + d_{\mathrm{av}}$$

with the 2-periodic function

$$d_0(t) = \begin{cases} -1, & \text{if } t \in [-1, 0) \\ 1, & \text{if } t \in [0, 1) \end{cases}$$

in which d_{av} is the average (residual) dispersion over one period and ε is a small parameter in a strong dispersion regime. By rescaling t to t/ε and averaging over the period, equation (1) is transformed into the following Gabitov–Turitsyn equation [10]

$$i\partial_t v + \varepsilon d_{\mathrm{av}} \nabla^2 v + \varepsilon \int_0^1 T_r^{-1}\big(|T_r v|^2\, T_r v\big) dr = 0, \tag{2}$$

where T_t is the solution operator of the free Schrödinger equation on $L^2(\mathbb{R}^n)$ for $n = 1, 2$. More precisely, $u(x,t) = (T_t f)(x)$ is the solution of the initial value problem

$$i\partial_t u = -\nabla^2 u \tag{3}$$

with $u(x, 0) = f(x)$, where x is a scalar variable in $\mathbb{R}$ and is a vector variable, $\mathbf{x} = (x_1, x_2)$, in $\mathbb{R}^2$. The averaging procedure from (1) to (2) was justified by Zharnitsky *et al.* in [32]. The usage of a standing wave with the ansatz $v(x,t) = e^{i\varepsilon\omega t} f(x)$ in (2) yields

$$-\omega f = -d_{\mathrm{av}} \nabla^2 f - \int_0^1 T_t^{-1}(|T_t f|^2 T_t f)\, dt \tag{4}$$

whose solution is called a dispersion managed soliton.

With the help of a variational principle, we can obtain an important functional

$$\inf\left\{ \frac{d_{\mathrm{av}}}{2} \|\nabla f\|_{L^2}^2 - \frac{1}{4}\int_0^1\int_{\mathbb{R}^n} |(T_t f)(x)|^4\, dx\, dt : \|f\|_{L^2}^2 = \lambda \right\} \tag{5}$$

related to (4) for $n = 1, 2$ which has been addressed in many mathematical studies as a constrained minimization problem. In the one-dimensional problem, (5) was used to show the existence of a weak solution for (4) in [32] and [17] when $d_{\mathrm{av}} > 0$ and $d_{\mathrm{av}} = 0$, respectively. It is not obvious to show that minimizers of (5) are smooth when $d_{\mathrm{av}} = 0$, while the case $d_{\mathrm{av}} > 0$ can be easily handled by bootstrapping, as in [13, 26, 32]. Moreover, it is shown that the weak solutions decay exponentially at infinity for both cases in [7, 11]. For further information, consult the review paper [28] and the references therein.

The two-dimensional case has also long been of interest to many researchers. In [32], Zharnitsky *et al.* proved the existence of minimizers to (5) for $n = 2$ as well. Kunze constructed a sequence of radially symmetric minimizers of (5) when $\omega > 0$ and $d_{\text{av}} > 0$ [15]. When $d_{\text{av}} = 0$, it was proved by Stanislavova that there can be no minimizers of (5) (see [26]).

Various numerical studies were performed to solve (1) and other versions of the equation, including (2) and (4), owing to the lack of known explicit forms of solutions to them [1,2,5,6,8,18–21,23,25,27,29–31]. Many approaches to the one-dimensional case utilized the pseudo-spectral schemes and the finite difference methods to obtain approximations for DM NLS. Taha *et al.* compared the results when explicit and implicit finite difference methods, a split step Fourier method, and a pseudo-spectral method were applied to DM NLS [27]. Chang *et al.* introduced two unique linearized Crank–Nicolson schemes to find approximations for DM NLS [5]. Zhang *et al.* used the Crank–Nicolson linear implicit scheme in their numerical simulations [8]. Delfour *et al.* presented a numerical solution of a modified DM NLS, including a dissipation term using a finite difference method [6] and a Sanz–Serna generalized Delfour's scheme [25]. In [25], the leap-frog technique and a modified Crank–Nicolson method were applied to the nonlinear Schrödinger equation. The scheme in [29] used the central difference formula in time and space derivatives. Xie *et al.* applied two compact finite difference schemes to one-dimensional NLS, which provided higher accuracy [31]. Wu performed DuFort–Frankel-type methods for linear and nonlinear Schrödinger equations [30]. Liu *et al.* showed a split step Fourier method that is fast in computing [18]. The Gabitov–Turitsyn equation model (2) has also been studied through numerical simulations for years. Ablowitz *et al.* addressed the $d_{\text{av}} = 1$ case in (2) and performed a numerical computation of the $d_{\text{av}} = 0$ case for (4) as well [2]. Lushnikov researched the same case in similar ways [19]. His other attempts to solve (4) numerically employed the fast Fourier transformation in $|d_{\text{av}}| \ll 1$ case [20, 21].

There are relatively few studies on higher dimensional problems than on one-dimensional ones. Abdullaev *et al.* dealt with (1) by using the two-dimensional fast Fourier transform [1]. Matuszewski *et al.* studied both the two-dimensional and the three-dimensional cases [23]. He focused on the stability region for the two cases and confirmed the unconditional instability for the three-dimensional case. Zharnitsky *et al.* verified the possibility of the existence of ground states by numerical computations when $d_{\text{av}} > 0$[33] in two dimensions.

Our objective is to find numerical eigenpairs (ω, f) of (4) with $d_{\text{av}} > 0$ and $d_{\text{av}} = 0$. Numerical studies stated above focus on getting f when ω is fixed. In this paper, we do not fix ω, if not necessary, but find both ω and f. The high order finite difference schemes, including Runge–Kutta fourth order method and fourth order centered scheme, are utilized in order to increase the accuracy of numerical solution and mesh/step sizes are carefully chosen to handle the numerical stability. We numerically verify the existence of nontrivial eigenpairs and explore how many of them exist. Note that if (ω, f) is an eigenpair corresponding to some d_{av}, then $(c\omega, \sqrt{c}f)$ is one corresponding to cd_{av} for any positive constant c. This implies that, for instance, if the L^2-norm of f is not restricted, then one can obtain infinitely many triples $(d_{\text{av}}, \omega, f)$

satisfying (4). We first prove this and then numerically verify it. Additionally, we show the convergence of ω and f when d_{av} approaches 0 in one-dimensional space as well as in two-dimensional space. Considering the result in [26], we can wonder if the two dimensional case with $d_{\text{av}} = 0$ can have a solution unlike the constrained minimization problem in [26]. Through the computation, we discover the possibility that this two dimensional problem can be solvable.

2. Numerical approximation to the nonlinear Schrödinger equation

This section is composed of two parts. First, we present an implementation of the solution operator T_t for the free Schrödinger equation (3). Then, we construct a numerical approximation of the problem (4). Here, the detailed techniques will only be described with a one-dimensional problem to ease understanding, as the notations are simpler. The overall process with the two-dimensional problem is analogous.

Considering equation (3) for $x \in \mathbb{R}$, the domain Ω is set as $\Omega = (-\alpha, \alpha) \times (0, 1)$ for sufficiently large $\alpha > 0$. Furthermore, we may assume that the equation holds the homogeneous Dirichlet boundary condition for u, $u(\pm\alpha, \cdot) = 0$, owing to the result that $f(x)$ decays exponentially as x tends to infinity [7]. The same strategy is applied to the two-dimensional problem by setting

$$\Omega = \left\{ \mathbf{x} = (x_1, x_2) \,|\, |\mathbf{x}| := \sqrt{x_1^2 + x_2^2} < \alpha \right\} \times (0, 1)$$

and by assuming $u(\mathbf{x}, \cdot) = 0$ when $|\mathbf{x}| = \alpha$.

2.1. Implementation of the operator T_t

Recall the free Schrödinger equation and the operator T_t in (3): let $u = T_t f$ be the solution to the following problem $i\partial_t u = -\partial_x^2 u$ with the initial condition $u(x, 0) = f(x)$. Throughout this paper, we set $\alpha = 20$ and confine t-interval to $(0, 1)$ with uniform discretization $(\Delta x, \Delta t)$, with mesh sizes of x and t, respectively. Let U_j^n be an approximation corresponding to $u(x_j, t_n)$ in which $(x_j, t_n) = (-\alpha + j\Delta x, n\Delta t)$ for $0 \le j \le M := 2\alpha/\Delta x,\ 0 \le n \le N := 1/\Delta t$. The Runge–Kutta fourth order method(RK4) is employed for $\partial_t u$-discretization and a fourth order central difference scheme is used for $\partial_x^2 u$-discretization such that

$$\partial_x^2 u(x_j, t_n) \approx D^2 U_j^n := \frac{(-U_{j-2}^n + 16U_{j-1}^n - 30U_j^n + 16U_{j+1}^n - U_{j+2}^n)}{12(\Delta x)^2}.$$

2.2. Numerical computation of (4)

Since the equation (4) is nonlinear, we utilize Picard iteration to identify a proper approximation of f. First the problem is transformed to the equivalent problem to solve $P(f) = 0$, where

$$P(f) = \omega f - d_{\text{av}} f'' - \int_0^1 T_t^{-1}(T_t f\ \overline{T_t f}\ T_t f)\ dt\ . \tag{6}$$

When one solves $P(f) = 0$ using Picard iteration, the system is first decomposed into linear and nonlinear parts such as $P(f) = Lf + N(f)$, where L is the linear operator, $Lf = \omega f - d_{\mathrm{av}} f''$, and N is the nonlinear operator. Then, it is solved iteratively

$$Lf^{(k+1)} = -N\left(f^{(k)}\right) \tag{7}$$

with given initial conditions $\omega^{(0)}$ and $f^{(0)}$. Hence, with the selected initial conditions $\omega^{(0)}$ and $f^{(0)}$, the implementation of the right hand side in (7) plays a key role in this paper. From now until (11), we omit the iteration index in the Picard iterative process '(k)' for notational simplicity and concentrate on the numerical implementation for

$$\int_0^1 T_t^{-1}(T_t f\ \overline{T_t f}\ T_t f)\ dt\ . \tag{8}$$

In Subsection 2.1, we found a numerical approximation $\mathbf{U} = (\mathbf{U}^n)_{n=1}^N$ of $u = T_t f$, where $\mathbf{U}^n = (U_j^n)$. That is, U_j^n is an approximation to $T_{t_n} f(x_j)$ with $t_n = n\Delta t$. To implement the integration (8), we use the composite trapezoidal rule as

$$\int_0^1 T_t^{-1}(T_t f\ \overline{T_t f}\ T_t f)dt = \sum_{n=1}^N \int_{t_{n-1}}^{t_n} T_t^{-1}(T_t f\ \overline{T_t f}\ T_t f)dt \approx \frac{\Delta t}{2} \sum_{n=1}^N (\mathbb{T}_{n-1} + \mathbb{T}_n)$$

in which $\mathbb{T}_m := T_{t_m}^{-1}\left(T_{t_m} f\, \overline{T_{t_m} f}\, T_{t_m} f\right)$.

We denote a matrix $\mathbf{W} = (\mathbf{W}^n)_{n=1}^N$ with $\mathbf{W}^n = \left(U_j^n \overline{U_j^n} U_j^n\right)_{j=0}^M$. Note that $T_{\Delta t}^{-1}$ can be computed by changing Δt as $(-\Delta t)$ in the RK4 in Subsection 2.1, see Chapter 2 in [12]. Thus, $(n-1)$-times of $T_{\Delta t}^{-1}$ is needed for $\mathbf{W}^n$ to get $\mathbb{T}_n$. For the discretization of the linear part, Lf, the fourth order central difference scheme introduced in Subsection 2.1 is used. Applying these two approximations above to (7) yields the next iterate $f^{(k+1)}$.

Assuming that $\omega \in \mathbb{C}$ and a nontrivial solution $f \in L^2(\mathbb{R})$ satisfy (4), then

$$\omega\langle f, f\rangle = d_{\mathrm{av}}\langle f, f''\rangle + \left\langle f, \int_0^1 T_t^{-1}\left(T_t f\ \overline{T_t f}\ T_t f\right) dt \right\rangle,$$

where $\langle g, f\rangle = \int_{\mathbb{R}} \overline{g(x)} f(x)\ dx$. Using the T_t's unitarity and integration by parts, we obtain the following equation which implies $\omega \in \mathbb{R}$ and provides $\omega^{(k+1)}$ when $f^{(k+1)}$ is obtained from $(\omega^{(k)}, f^{(k)})$:

$$\omega\|f\|_{L^2}^2 = -d_{\mathrm{av}}\|f'\|_{L^2}^2 + \int_0^1 \int_{\mathbb{R}} |T_t f|^4\ dx\ dt\ . \tag{9}$$

Hereafter, we use the subindex omitted notation $\|\cdot\|$ for the L^2-norm to simplify the notation. Note that our desired ω must satisfy the following properties.

For the one-dimensional problem,

$$\int_0^1 \int_{\mathbb{R}} |T_t f|^4 \ dx\ dt \le \left(\int_0^1 \int_{\mathbb{R}} |T_t f|^6 \ dx\ dt \right)^{\frac{3}{6}} \left(\int_0^1 \int_{\mathbb{R}} |T_t f|^2 \ dx\ dt \right)^{\frac{1}{2}}$$
$$\le \left(12^{-\frac{1}{12}} \|f\| \right)^3 \|f\| .$$

The value $12^{-1/12}$ in the last inequality was discovered by Hundertmark and Zharnitsky [14] and by Foschi [9]. Combining this inequality with (9) yields

$$\omega \le 12^{-\frac{1}{4}} \|f\|^2 . \tag{10}$$

We obtain another estimate for the last term in (9) as

$$\int_0^1 \int_{\mathbb{R}} |T_t f|^4 \ dx\ dt \le \frac{1}{\sqrt{3}} \|f'\| \, \|f\|^3$$

by using an inequality of Sobolev type (see [32] for more details). Then, through a simple calculation, one can see $\omega \le \|f\|^4/(12 d_{\mathrm{av}})$. Note that this bound is less sharp (larger upper bound) than the one given in (10) when $d_{\mathrm{av}} \le \|f\|^2/(12^{3/4})$.

The overall Picard iteration stops when it satisfies

$$\|f^{(k)} - f^{(k+1)}\|_{l^2} / \|f^{(k+1)}\|_{l^2} < \varepsilon \ll 1, \tag{11}$$

where $\|\cdot\|_{l^2}$ is the discrete l^2-norm. Finally, $f^{(k+1)}$ is the proposed approximation to (4).

The two-dimensional case framework and all numerical processes are very analogous to the one-dimensional case. Only the numerical calculation for ∂_x^2 needs to be changed to a numerical calculation for Laplacian, ∇^2. There are also similar known theories regarding the upper bound of ω associated with f. For instance, Hundertmark *et al.* (see [14]) and Carneiro (see [4]) had shown respectively

$$\omega \le \|f\|^2/4 \quad \text{ and } \omega \le \|f\|^4/(64\,\pi\, d_{\mathrm{av}}).$$

3. Numerical results

In this section, the results of the proposed numerical computations are presented. These results first justify known theoretical facts mentioned in Section 1 and then show some evidence that can provide possibilities to resolve unknown or unsolved problems. In particular, the following two dimensional open problems are of our special interest: the behavior of eigenpairs when $d_{\mathrm{av}} \to 0$ and the existence of them for the zero average dispersion case.

We use three types of functions as the initial guesses for $\mathbf{x} := x \in \mathbb{R}$ and $\mathbf{x} \in \mathbb{R}^2$: $\exp(-|\mathbf{x}|^2/2)$, $\cos(|\mathbf{x}|^2/16)\exp(-|\mathbf{x}|)$, and $\sum_{q=1}^m a_q \mathrm{sech}\,(x + b_q)$. We choose different constants (a_m, b_m) for the last type initial guess to vary the number of humps and to control the symmetry. Since our interest lies in finding an eigenpair (ω, f) for an arbitrary $d_{\mathrm{av}} \ge 0$, the numerical simulations with various d_{av} values have been performed. In the one-dimensional problem, both the x-mesh size Δx and t-mesh size Δt are set to 0.05 and 0.001, respectively, over the considering domain $[-20, 20] \times [0, 1]$. We perform the iterations until the tolerance ε of relative error (11) becomes sufficiently small. For each iteration, $f^{(k)}$ is normalized to avoid obtaining a meaningless approximation close to zero. Numerical computations for the two dimensional case are conducted by choosing $\alpha = 6$ as the radius of the domain and using the same iterative process of the one-dimensional case. Note that $(\omega_g, f_g), (\omega_c, f_c)$ and (ω_s, f_s) in the following subsections indicate that the results when initial guesses are chosen as $\exp(-|\mathbf{x}|^2/2)$, $\cos(|\mathbf{x}|^2/16)\exp(-|\mathbf{x}|)$, and $\sum_{q=1}^{m} a_q \operatorname{sech}(x + b_q)$, respectively.

3.1. $d_{\rm av} > 0$ case

When $d_{\rm av} > 0$, the existence of a weak solution to the problem (4) is well-known [32]. In addition to the weak solution existence theory, for cases where f is a minimizer of the corresponding variational problem (5), the fast decay was guaranteed in [11] and regularity was verified mathematically in [13, 26, 32]. Our numerical solutions show similar fast decaying behavior (see Figures 1-3, 8). Note that symmetric initial guesses lead us to even eigenfunctions, and non-symmetric initial guesses chosen as a linear combination of hyperbolic secant functions generate eigenfunctions with axis of symmetry $x = r \neq 0$ (see Figures 1-3, 8). Oscillatory motion has been observed in other literatures as well (see [19–21]). In our results, the oscillatory behavior of eigenfunctions is only observed for small $d_{\rm av}$ which is when $d_{\rm av} \leq 10^{-2}$. It is more clearly shown through the graphs of $\log(|f|)$ (see Figure 5). As $d_{\rm av}$ gets smaller (here $d_{\rm av} \leq 10^{-2}$), oscillation happens away from $x = 0$, as seen in Figure 4-(A), and if $d_{\rm av}$ is small enough ($d_{\rm av} \leq 10^{-6}$), then eigenfunctions have little difference, as seen in Figure 4-(B). Nonlinearity is expected to be a cause of such oscillation.

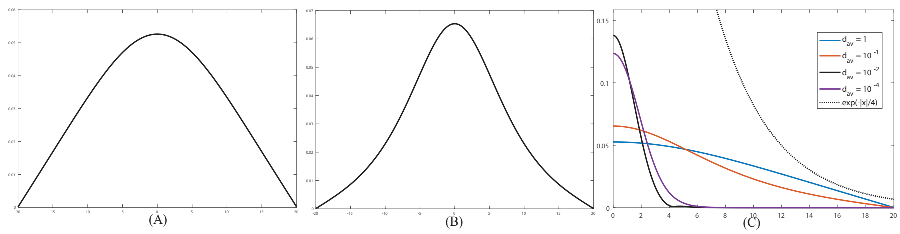

FIGURE 1. $|f_g|$ graphs (A) $d_{\rm av} = 1$ (B) $d_{\rm av} = 0.1$ (C) Exponential decay of solutions

As briefly addressed in the introduction, if (ω, f) is an eigenpair corresponding to some $d_{\rm av}$, then one can easily prove that $(c\omega, \sqrt{c}f)$ is an eigenpair for $cd_{\rm av}$ for any positive constant c such as

$$c\omega(\sqrt{c}f) - cd_{\rm av}\nabla^2(\sqrt{c}f) - \int_0^1 T_t^{-1}\Big(\big|T_t(\sqrt{c}f)\big|^2\, T_t(\sqrt{c}f)\Big)\, dt$$

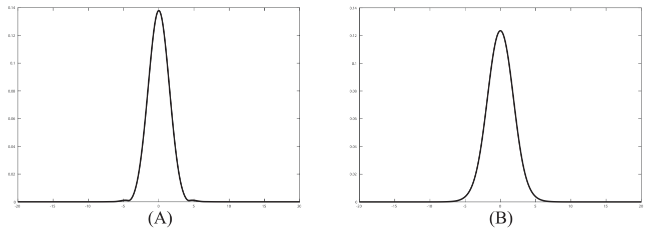

FIGURE 2. $|f_c|$ graphs (A) $d_{\text{av}} = 10^{-2}$ (B) $d_{\text{av}} = 10^{-4}$

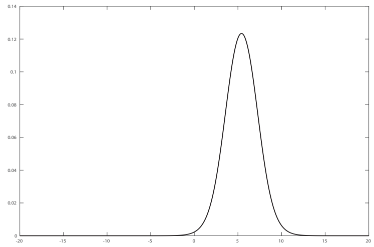

FIGURE 3. $|f_s|$, $d_{\text{av}} = 10^{-4}$ with a non-symmetric initial guess

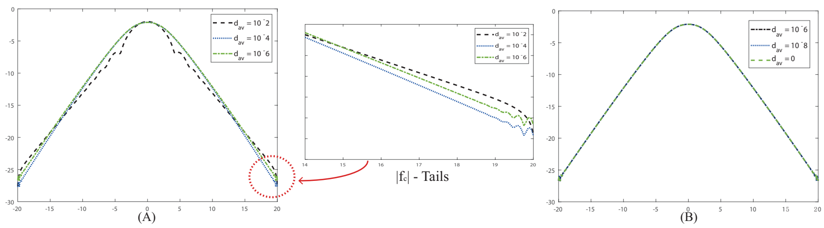

FIGURE 4. $\log(|f_c|)$ graphs (A) $d_{\text{av}} = 10^{-2}, 10^{-4}, 10^{-6}$ (B) $d_{\text{av}} = 10^{-6}, 10^{-8}, 0$

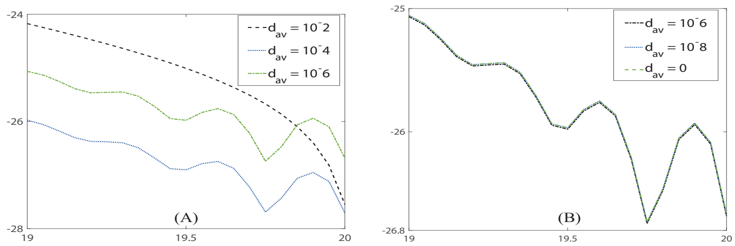

FIGURE 5. Oscillation of tail (A) $d_{\text{av}} = 10^{-2}, 10^{-4}, 10^{-6}$ (B) $d_{\text{av}} = 10^{-6}, 10^{-8}, 0$

$$= c\sqrt{c}\left\{\omega f - d_{\text{av}}\nabla^2 f - \int_0^1 T_t^{-1}(|T_t f|^2\, T_t f)dt\right\}. \tag{12}$$

We confirm the fact above through numerical tests as well. For example, for $d_{\text{av}} = 10^{-3}$, we obtain $\tilde{\omega} = 0.020506$ and $\tilde{f}$ with the Gaussian initial guess. Then, if we run the numerical simulation again with $d_{\text{av}} = 10^{-2}$ and L^2-norm fixed as $\sqrt{10}$-time $\|\tilde{f}\|_{L^2}$ in the normalization, then the results are $\omega = 0.20506 \approx 10\tilde{\omega}$ and f with $\|f - \sqrt{10}\tilde{f}\|_{L^2} < 10^{-5}$.

In the two-dimensional problem, Kunze found a sequence $\{u_j\}$ of radially symmetric minimizers with the same L^2-norm. Our two-dimensional numerical test result also yields radial symmetry solutions, which supports Kunze's result; see Figure 6.

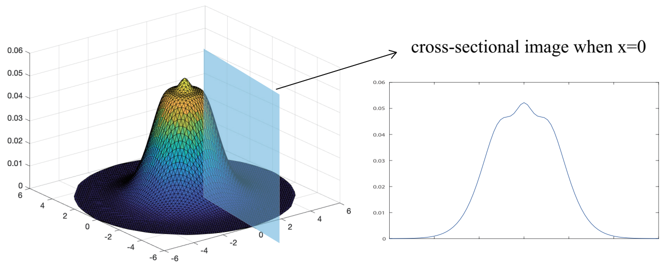

FIGURE 6. Resulting $|f_g|$ for the 2D case when $d_{\text{av}} = 10^{-4}$

3.2. $d_{\text{av}} = 0$ case

The existence of a weak solution of the problem (4) in this case for one dimension was proved by Kunze, and the exponential decay of weak solutions was shown by Erdoğan *et al.* in [7]. The results of our numerical simulations verify these mathematical theories. Moreover, our proposed numerical scheme allows us to update (ω, f) simultaneously without fixing either ω or f in an iterative manner (see Table 1 and Figure 8).

TABLE 1. Computed ω in 1D

d_{av}	10^{-1}	10^{-2}	10^{-4}	10^{-8}	0
ω_g	0.0027	0.0148	0.0211	0.0211	0.0211
ω_c	0.0027	0.0148	0.0211	0.0211	0.0211
ω_s	0.0027	0.0148	0.0211	0.0211	0.0211

In [26], Stanislavova verified the nonexistence of minimizers in the two-dimensional case by proving that (5) with $d_{\text{av}} = 0$ cannot be achieved by any f. This result is very important to understand the equation (4) when $d_{\text{av}} = 0$,

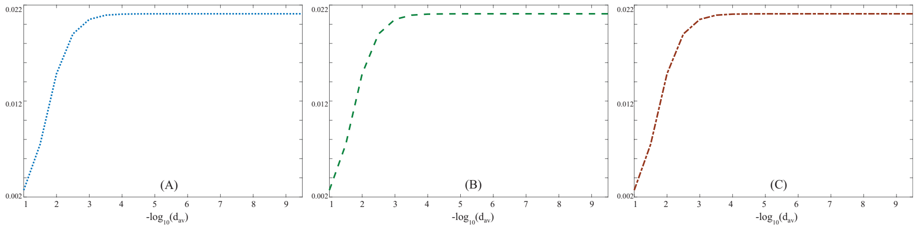

FIGURE 7. (A) ω_g (B) ω_c and (C) ω_s values as $d_{av} \to 0$

however, it does not imply that (4) has only the trivial solution. Through our computation, we found that there can be a nontrivial solution to (4), which has radial symmetry and fast decay when it is not confined to be a minimizer, as in Figure 9.

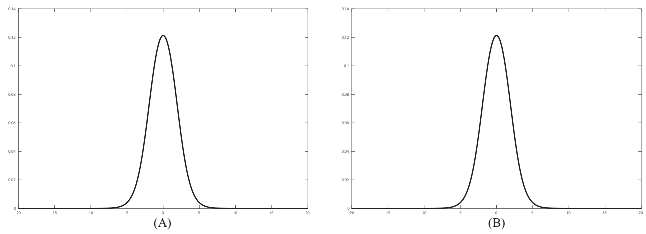

FIGURE 8. f_g and f_c when $d_{\text{av}} = 0$ (A) $|f_g|$ (B) $|f_c|$

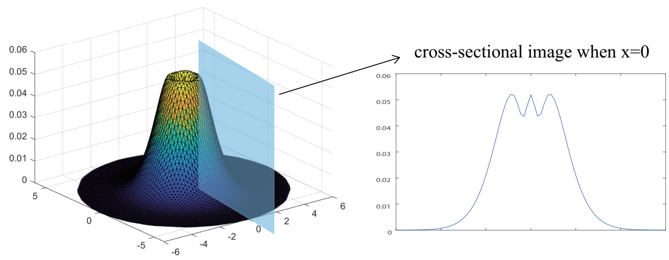

FIGURE 9. $|f_g|$ for the 2D case when $d_{\text{av}} = 0$

3.3. $d_{\text{av}} \to 0$ observation

One of our objectives is to observe the behavior of the eigenpairs as $d_{\text{av}} \to 0$ to see if the characteristics associated to (ω, f) with $d_{\text{av}} > 0$ continuously converge to the ones with $d_{\text{av}} = 0$. For each initial guess, we select various d_{av}

values that are approaching 0 and construct a sequence $\{d_{\text{av}}^m\}$ with $d_{\text{av}}^m \to 0$ as $m \to \infty$. Let (ω_m, f_m) be an eigenpair corresponding to d_{av}^m for each $m \in \mathbb{N}$ and let (ω, f) be an eigenpair for $d_{\text{av}} = 0$. As long as we obtain f_m for $m \in \mathbb{N}$ and f from the same initial guess, the result shows that $\omega_m \to \omega$ in $\mathbb{R}$ (see Table 1 and Figure 7) and $f_m \to f$ in L^2, as $m \to \infty$ (see Figure 4-(B) and 5-(B)). Kunze mathematically proved a similar behavior though he only addressed a one-dimensional constrained minimization problem [16]. Based on the numerical results, we may claim that this converging behavior need not be restricted on a constrained minimization problem. To the best of our knowledge, there are no theoretical proofs that show this continuous behavior with d_{av} approaching 0 in two dimensions. In this paper, we present the numerical evidence that Kunze's conclusion in [16] can be true in the two dimensional problem as well.

4. Conclusion

The presented numerical results support important mathematical theories for various d_{av} that had been known for years. On the other hand, some of our numerical solutions diverged from previous mathematically described characteristics that are considered in the problems addressing minimizers as our simulations are not constrained to deal with minimizers. For $d_{\text{av}} > 0$, our computation proves that there can be infinitely many eigenpairs corresponding to each d_{av}. When d_{av} is fixed, ω is found as a unique value and the corresponding eigenfunctions have only different axis of symmetry depending on the symmetry of initial guesses. For the two-dimensional problem, an observation through numerical simulations leads us to interesting findings that imply the possible existence of a solution to the $d_{\text{av}} = 0$ case, which has not been theoretically verified previously. Because it turned out that there are no minimizers of the same problem by Stanislavova [26], we believe that this result can be very meaningful for some applications. The result of the $d_{\text{av}} \to 0$ case intimates that there can be a way to construct a sequence of eigenpairs converging to an eigenpair for the $d_{\text{av}} = 0$ case, even if the problem was solved in a variational problem (5) in [16]. It can be also valid for the two-dimensional case considering the results of our two-dimensional simulations. If we combine this convergent behavior with the result of (12), we can also claim that there exists a sequence of eigenpairs convergent to (ω, f) where (ω, f) is an arbitrary eigenpair corresponding to $d_{\text{av}} = 0$. Hence, we conclude that there can be many challenging mathematical problems related to (1) if one does not restrict them to minimization problems.

References

[1] F. Kh. Abdullaev, B. B. Baizakov, and M. Salerno, *Stable two-dimensional dispersion-managed soliton*, Phys. Rev. E **68** (2003), 00605, 1–4.

[2] M. J. Ablowitz and G. Biondini, *Multiscale pulse dynamics in communication systems with strong dispersion management*, Opt. Lett. **23** (1998), 1668–1670.

[3] J. Bonetti, N. Linale, A. D. Sanchez, S. M. Hernandez, P. I. Fierens, and D. F. Grosz, *Modified nonlinear Schrödinger equation for frequency-dependent nonlinear profiles of arbitrary sign*, J. Opt. Soc. Am. B **36** (2019), 3139–3144.
[4] E. Carneiro, *A sharp inequality for the Strichartz norm*, Int. Math. Res. Not. IMRN **2009** (2009), no. 16, 3127–3145. `https://doi.org/10.1093/imrn/rnp045`
[5] Q. Chang, E. Jia, and W. Sun, *Difference schemes for solving the generalized nonlinear Schrödinger equation*, J. Comput. Phys. **148** (1999), no. 2, 397–415. `https://doi.org/10.1006/jcph.1998.6120`
[6] M. Delfour, M. Fortin, and G. Payre, *Finite-difference solutions of a nonlinear Schrödinger equation*, J. Comput. Phys. **44** (1981), no. 2, 277–288. `https://doi.org/10.1016/0021-9991(81)90052-8`
[7] M. B. Erdoğan, D. Hundertmark, and Y.-R. Lee, *Exponential decay of dispersion managed solitons for vanishing average dispersion*, Math. Res. Lett. **18** (2011), no. 1, 11–24. `https://doi.org/10.4310/MRL.2011.v18.n1.a2`
[8] Z. Fei, V. M. Pérez-García, and L. Vázquez, *Numerical simulation of nonlinear Schrödinger systems: a new conservative scheme*, Appl. Math. Comput. **71** (1995), no. 2-3, 165–177. `https://doi.org/10.1016/0096-3003(94)00152-T`
[9] D. Foschi, *Maximizers for the Strichartz inequality*, J. Eur. Math. Soc. (JEMS) **9** (2007), no. 4, 739–774. `https://doi.org/10.4171/JEMS/95`
[10] I. Gabitov and S. K. Turitsyn, *Averaged pulse dynamics in a cascaded transmission system with passive dispersion compensation*, Opt. Lett. **21** (1996), 327–329.
[11] W. R. Green and D. Hundertmark, *Exponential decay of dispersion-managed solitons for general dispersion profiles*, Lett. Math. Phys. **106** (2016), no. 2, 221–249. `https://doi.org/10.1007/s11005-015-0811-9`
[12] W. G. Hoover and C. G. Hoover, *Time reversibility, computer simulation, algorithms, chaos*, second edition, Advanced Series in Nonlinear Dynamics, 13, World Scientific Publishing Co. Pte. Ltd., Hackensack, NJ, 2012. `https://doi.org/10.1142/8344`
[13] D. Hundertmark and Y.-R. Lee, *Decay estimates and smoothness for solutions of the dispersion managed non-linear Schrödinger equation*, Comm. Math. Phys. **286** (2009), no. 3, 851–873. `https://doi.org/10.1007/s00220-008-0612-4`
[14] D. Hundertmark and V. Zharnitsky, *On sharp Strichartz inequalities in low dimensions*, Int. Math. Res. Not. **2006** (2006), Art. ID 34080, 18 pp. `https://doi.org/10.1155/IMRN/2006/34080`
[15] M. Kunze, *Infinitely many radial solutions of a variational problem related to dispersion-managed optical fibers*, Proc. Amer. Math. Soc. **131** (2003), no. 7, 2181–2188. `https://doi.org/10.1090/S0002-9939-02-06780-1`
[16] ______, *The singular perturbation limit of a variational problem from nonlinear fiber optics*, Phys. D **180** (2003), no. 1-2, 108–114. `https://doi.org/10.1016/S0167-2789(03)00066-6`
[17] ______, *On a variational problem with lack of compactness related to the Strichartz inequality*, Calc. Var. Partial Differential Equations **19** (2004), no. 3, 307–336. `https://doi.org/10.1007/s00526-003-0218-9`
[18] X. Liu and B. Lee, *A fast method for nonlinear Schrödinger equation*, IEEE Photon. Technol. Lett. **15** (2003), 1549–1551.
[19] P. M. Lushnikov, *Dispersion-managed soliton in optical fibers with zero average dispersion*, Opt. Lett. **25** (2000), 1144–1146.
[20] ______, *Dispersion-managed soliton in a strong dispersion map limit*, Opt. Lett. **26** (2001), 1535–1537.
[21] ______, *Oscillating tails of dispersion managed soliton*, J. Opt. Soc. Am. B **21** (2004), 1913–1918.
[22] O. V. Marchukov, B. A. Malomed, V. A. Yurovsky, M. Olshanii, V. Dunjko, and R. G. Hulet, *Splitting of nonlinear-Schrödinger-equation breathers by linear and nonlinear*

localized potentials, Phys. Rev. A **99** (2019), no. 6, 063623, 11 pp. https://doi.org/10.1103/physreva.99.063623

[23] M. Matuszewski, M. Trippenbach, B. A. Malomed, E. Infeld, and A. A. Skorupski, *Two-dimensional dispersion-managed light bullets in Kerr media*, Phys. Rev. E **70** (2004), 016603 1–6.

[24] L. F. Mollenauer, A. Grant, X. Liu, X. Wei, C. Xie, and I. Kang, *Experimental test of dense wavelength-division multiplexing using novel, periodic-group-delay-complemented dispersion compensation and dispersion-managed solitons*, Opt. Lett. **28** (2003), 2043–2045.

[25] J. M. Sanz-Serna, *Methods for the numerical solution of the nonlinear Schroedinger equation*, Math. Comp. **43** (1984), no. 167, 21–27. https://doi.org/10.2307/2007397

[26] M. Stanislavova, *Regularity of ground state solutions of dispersion managed nonlinear Schrödinger equations*, J. Differential Equations **210** (2005), no. 1, 87–105. https://doi.org/10.1016/j.jde.2004.10.006

[27] T. R. Taha and M. J. Ablowitz, *Analytical and numerical aspects of certain nonlinear evolution equations. II. Numerical, nonlinear Schrödinger equation*, J. Comput. Phys. **55** (1984), no. 2, 203–230. https://doi.org/10.1016/0021-9991(84)90003-2

[28] S. K. Turitsyn, B. G. Bale, and M. P. Fedoruk, *Dispersion-managed solitons in fibre systems and lasers*, Phys. Rep. **521** (2012), no.4, 135–203.

[29] E. H. Twizell, A. G. Bratsos, and J. C. Newby, *A finite-difference method for solving the cubic Schrödinger equation*, Math. Comput. Simulation **43** (1997), no. 1, 67–75. https://doi.org/10.1016/S0378-4754(96)00056-0

[30] L. Wu, *Dufort-Frankel-type methods for linear and nonlinear Schrödinger equations*, SIAM J. Numer. Anal. **33** (1996), no. 4, 1526–1533. https://doi.org/10.1137/S0036142994270636

[31] S.-S. Xie, G.-X. Li, and S. Yi, *Compact finite difference schemes with high accuracy for one-dimensional nonlinear Schrödinger equation*, Comput. Methods Appl. Mech. Engrg. **198** (2009), no. 9-12, 1052–1060. https://doi.org/10.1016/j.cma.2008.11.011

[32] V. Zharnitsky, E. Grenier, C. K. R. T. Jones, and S. K. Turitsyn, *Stabilizing effects of dispersion management*, Phys. D **152/153** (2001), 794–817. https://doi.org/10.1016/S0167-2789(01)00213-5

[33] V. Zharnitsky, E. Grenier, S. K. Turitsyn, C. K. R. T. Jones, and J. S. Hesthaven, *Ground states of dispersion-managed nonlinear Schrödinger equation*, Phys. Rev. E (3) **62** (2000), no. 5, part B, 7358–7364. https://doi.org/10.1103/PhysRevE.62.7358

Younghoon Kang
Department of Mathematics
Sogang University
Seoul 04107, Korea
Email address: kkyh0409@gmail.com

Eunjung Lee
Department of Computational Science and Engineering
Yonsei University
Seoul 03722, Korea
Email address: eunjunglee@yonsei.ac.kr

Young-Ran Lee
Department of Mathematics
Sogang University
Seoul 04107, Korea
Email address: younglee@sogang.ac.kr